

Reactivity Studies, Structural Characterization, and Thermolysis of Cubic Titanosiloxanes: Precursors to Titanosilicate Materials Which Catalyze Olefin Epoxidation[†]

Ramaswamy Murugavel,* Paul Davis, and Vivekanand S. Shete

Department of Chemistry, Indian Institute of Technology—Bombay, Powai, Mumbai-400 076, India

Received March 25, 2003

The cubic titanosiloxane $[\text{RSiO}_3\text{Ti}(\text{OPr})]_4$ ($\text{R} = 2,6\text{-Pr}_2\text{C}_6\text{H}_3\text{NSiMe}_3$) (**1**) is found to be relatively inert in its attempted reactions with alcohols and other acidic hydrogen containing compounds. The reaction of **1** with silanol $(\text{Bu}^t\text{O})_3\text{-SiOH}$ however proceeds over a period of approximately 3 months to result in the hydrolysis of $(\text{Bu}^t\text{O})_3\text{SiOH}$ and yield the transesterification product $[\text{RSiO}_3\text{Ti}(\text{OBu}^t)]_4$ (**2**) rather than the expected $[\text{RSiO}_3\text{Ti}(\text{OSi}(\text{OBu}^t)_3)]_4$. Products **1** and **2** have been characterized by elemental analysis, thermal analysis, and spectroscopic techniques (IR, EIMS, and NMR). The solid-state structures of both **1** and **2** have been determined by single-crystal X-ray diffraction studies. Compounds **1** and **2** are isomorphous and crystallize in a cubic space group with a central cubic $\text{Ti}_4\text{Si}_4\text{O}_{12}$ core. Solid state thermolysis of **1** was carried at 450, 600, 800, 900, 1000, and 1200 °C in air, and the resulting titanosilicate materials **1a–f** were characterized by spectroscopic (IR and DR UV), powder XRD, and electron microscopic methods. While, the presence of Ti–O–Si linkages appears to be dominant in the samples prepared at lower temperatures (450–800 °C), phase separation of anatase and rutile forms of TiO_2 occurs at temperatures above 900 °C as revealed by IR spectral and PXRD studies. The presence of octahedral titanium centers was observed by DR UV spectroscopy for the samples heated at higher temperatures. The use of new titanosilicate materials as catalysts for olefin epoxidation has been investigated. The titanosilicate materials produced at temperatures below 800 °C with a large number of Ti–O–Si linkages (or tetrahedral titanium centers) were found to be more active catalysts compared to the materials produced above 900 °C. The observed conversion in the epoxidation reactions was found to be somewhat low although the selectivity of the epoxide formation over the other possible oxidized products was found to be very good.

Introduction

Silicon–oxygen linkage is the most common chemical bond in nature, and the heterosiloxane linkage is the most prominent structural moiety in silicate materials.¹ Silanols containing one or more –OH groups on silicon² have been extensively used in the synthesis of heterosiloxanes which have utility both as model compounds for larger silicate structures^{3–8} and as single-source precursors for silicate

materials.⁹ Different approaches have been employed by various workers in this area to achieve this goal. For example, it is possible to tailor the silicon:metal ratio in these systems

* To whom correspondence should be addressed. E-mail: rmv@iitb.ac.in. Fax: +(22) 2572 3480. Tel: +(22) 2576 7163.

[†] Dedicated to Professor C. N. R. Rao on the occasion of his 70th birthday.

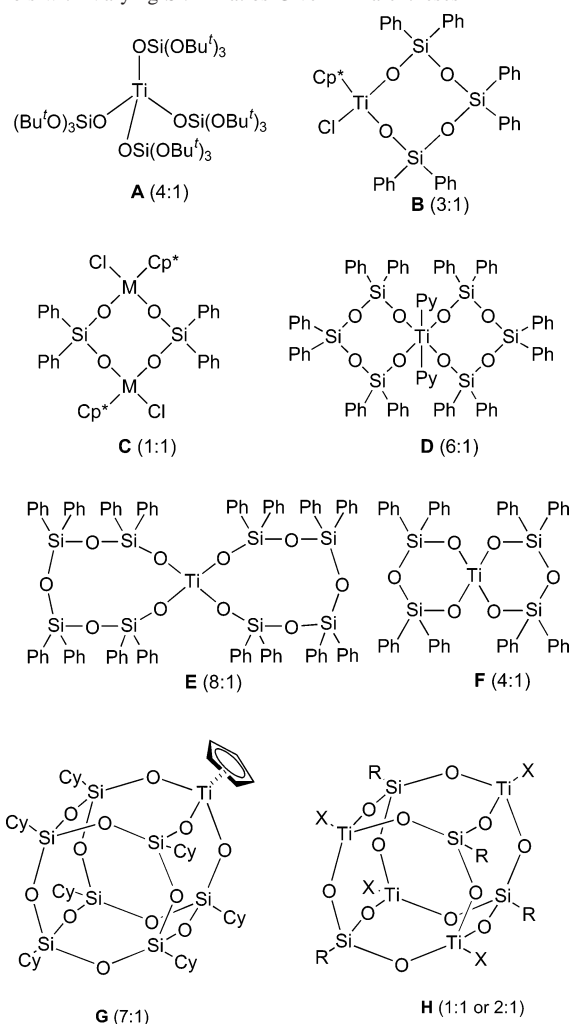
- (1) Walawalkar, M. G.; Murugavel, R.; Roesky, H. W. *Tailor made Silicon Oxygen Compounds-From Molecules to Materials*; Corriu, R., Jutzi, P., Eds.; Vieweg: Braunschweig, Germany, 1996; p 61.
- (2) (a) Lickiss, P. D. *Adv. Inorg. Chem.* **1995**, *42*, 147. (b) Murugavel, R.; Chandrasekhar, V.; Voigt, A.; Roesky, H. W.; Schmidt, H.-G.; Noltenmeyer, M. *Organometallics* **1995**, *14*, 5298.

- (3) (a) Murugavel, R.; Voigt, A.; Walawalkar, M. G.; Roesky, H. W. *Chem. Rev.* **1996**, *96*, 2205. (b) Murugavel, R.; Chandrasekhar, V.; Roesky, H. W. *Acc. Chem. Res.* **1996**, *29*, 183.
- (4) Beckmann, J.; Jurkschat, K. *Coord. Chem. Rev.* **2001**, *215*, 267.
- (5) (a) Lorenz, V.; Fischer, A.; Giessmann, S.; Gilje, J. W.; Gun'ko, Y.; Jacob, K.; Edelmann, F. T. *Coord. Chem. Rev.* **2000**, *206–207*, 321. (b) King, L.; Sullivan, A. C. *Coord. Chem. Rev.* **1999**, *189*, 19.
- (6) Feher, F. J.; Budzichowski, T. A. *Polyhedron* **1995**, *14*, 3239.
- (7) Duchateau, R. *Chem. Rev.* **2002**, *102*, 3525.
- (8) Abbenhuis, H. C. L. *Chem.—Eur. J.* **2000**, *6*, 25.
- (9) (a) Furdala, K. L.; Oliver, A. G.; Hollander, F. J.; Tilley, T. D. *Inorg. Chem.* **2003**, *42*, 1140. (b) Brutchey, R. L.; Goldberger, J. E.; Koffas, T. S.; Tilley, T. D. *Chem. Mater.* **2003**, *15*, 1040. (c) Tilley, T. D. *J. Mol. Catal., A* **2002**, *182–183*, 17. (d) Furdala, K. L.; Tilley, T. D. *Chem. Mater.* **2002**, *14*, 1376. (e) Lugmair, C. G.; Furdala, K. L.; Tilley, T. D. *Chem. Mater.* **2002**, *14*, 888. (f) Furdala, K. L.; Tilley, T. D. *J. Am. Chem. Soc.* **2001**, *123*, 10133. (g) Kriesel, J. W.; Sander, M. S.; Tilley, T. D. *Adv. Mater.* **2001**, *13*, 331.

by suitably choosing a silanol with the desired number of hydroxyl groups.

The reactions of silanols (such as R_3SiOH , $R_2Si(OH)_2$, $RSi(OH)_3$) with a series of titanium alkoxides, alkyls, halides, and amides have been investigated very intensively with the aim to produce model compounds for well-known Ti-based silicate and silicalite materials,^{10a} which show interesting catalytic applications in several organic transformations including oxidation of olefins to epoxides.¹⁰ The range of titanosiloxanes that have been synthesized thus far using a molecular approach show very interesting silicon-to-titanium ratio in the final products obtained (Chart 1).^{9a,11–14,15a} Particularly interesting among these are the cubic titanosiloxanes **G**^{14a} and **H**^{13a} which have been derived from

Chart 1. Molecular Titanosiloxanes Derived from Different Types of Silanols with Varying Si:Ti Ratios Given in Parentheses

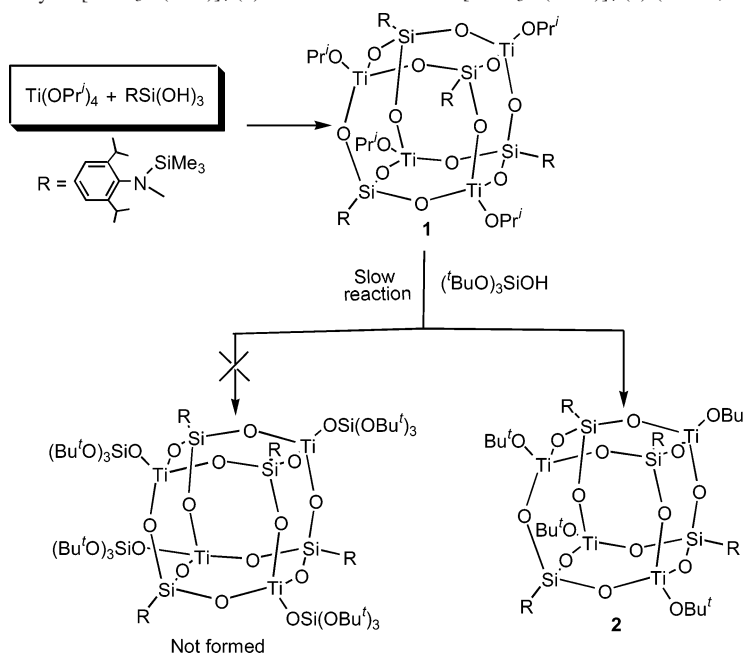


- (10) (a) Murugavel, R.; Roesky, H. W. *Angew. Chem., Int. Ed. Engl.* **1997**, *36*, 477. (b) Laha, S. C.; Kumar, R. *J. Catal.* **2002**, *208*, 339. (c) Wang, X.-S.; Guo, X. W.; Li, G. *Catal. Today* **2002**, *74*, 65. (d) Laha, S. C.; Kumar, R. *J. Catal.* **2001**, *204*, 64. (e) Schmidt, I.; Krogh, A.; Wienberg, K.; Carlsson, A.; Brorson, M.; Jacobsen, C. J. H. *Chem. Commun.* **2000**, 2157. (f) Bhaumik, A.; Tatsumi, T. *Chem. Commun.* **1998**, 463.
- (11) (a) Horacek, M.; Stepnicka, P.; Kubista, J.; Gyepes, R.; Cisarova, I.; Petrusova, L.; Mach, K. *J. Organomet. Chem.* **2002**, *658*, 235. (b) Hofmann, M.; Malisch, W.; Schumacher, D.; Lager, M.; Nieger, M. *Organometallics* **2002**, *21*, 3485. (c) Sobota, P.; Przybylak, S.; Ejfler, J.; Kobylka, M.; Jerzykiewicz, L. B. *Inorg. Chim. Acta* **2002**, *334*, 159. (d) Zemanek, J.; Horacek, M.; Thewalt, U.; Stepnicka, P.; Kubista, J.; Cejka, J.; Petrusova, L.; Mach, K. *Inorg. Chem. Commun.* **2001**, *4*, 520. (e) Dell'Amico, D. B.; Calderazzo, F.; Ianelli, S.; Labella, L.; Marchetti, F.; Pelizzi, G. *J. Chem. Soc., Dalton Trans.* **2000**, 4339. (f) Johnson, B. F. G.; Klunduk, M. C.; Martin, C. M.; Sankar, G.; Teate, S. J.; Thomas, J. M. *J. Organomet. Chem.* **2000**, *596*, 221. (g) Ciruelos, S.; Cuenca, T.; Gomez-Sal, P.; Manzanero, A.; Royo, P. *Organometallics* **1995**, *14*, 177.
- (12) (a) Murugavel, R.; Shete, V. S.; Baheti, K.; Davis, P. *J. Organomet. Chem.* **2001**, *625*, 195. (b) Voigt, A.; Murugavel, R.; Montero, M. L.; Wesel, H.; Liu, F.-Q.; Roesky, H. W.; Usón, I.; Albers, T.; Parisini, E. *Angew. Chem., Int. Ed. Engl.* **1997**, *36*, 1001. (c) Beckmann, J.; Jurkschat, K.; Müller, D.; Rabe, S.; Schürmann, M. *Organometallics* **1999**, *18*, 2326. (d) Höbbel, D.; Nacken, M.; Schmidt, H.; Huch, V.; Veith, M. *J. Mater. Chem.* **1998**, *8*, 171. (e) Lazell, M.; Motevalli, M.; Shah, S. A. A.; Simon, C. K. S.; Sullivan, A. C. *J. Chem. Soc., Dalton Trans.* **1996**, 1449. (f) Hossain, M. A.; Hursthouse, M. B.; Ibrahim, A.; Mazid, M.; Sullivan, A. C. *J. Chem. Soc., Dalton Trans.* **1989**, 2347. (g) Hossain, M. A.; Hursthouse, M. B.; Mazid, M. A.; Sullivan, A. C. *J. Chem. Soc., Chem. Commun.* **1988**, 1305. (h) Fandos, R.; Otero, A.; Rodriguez, A.; Ruiz, M. J.; Terreros, P. *Angew. Chem., Int. Ed.* **2001**, *40*, 2884. (i) Liu, F.-Q.; Schmidt, H. G.; Noltemeyer, M.; Freire-Erdbrügger, C.; Sheldrick, G. M.; Roesky, H. W. *Z. Naturforsch.* **1992**, *47B*, 1085. (j) Haouadi-Mazzah, A.; Mazzah, A.; Schmidt, H. G.; Noltemeyer, M.; Roesky, H. W. *Z. Naturforsch.* **1991**, *46B*, 587. (k) Haouadi, A.; Dhamelincourt, P.; Mazzah, A.; Drache, M.; Conflant, P.; Lazraq, M. *J. Mater. Chem.* **2000**, 1001.
- (13) (a) Voigt, A.; Murugavel, R.; Chandrasekhar, V.; Winkhofer, N.; Roesky, H. W.; Schmidt, H.-G.; Usón, I. *Organometallics* **1996**, *15*, 1610. (b) Winkhofer, N.; Voigt, A.; Dorn, H.; Roesky, H. W.; Steiner, A.; Stalke, D.; Reller, A. *Angew. Chem., Int. Ed. Engl.* **1994**, *33*, 1352. (c) Lindemann, H. M.; Schneider, M.; Neumann, B.; Stämmler, H.-G.; Stämmler, A.; Jutzli, P. *Organometallics* **2002**, *21*, 3009. (d) Nolte, J. O.; Schneider, M.; Neumann, B.; Stämmler, H. G.; Jutzli, P. *Organometallics* **2003**, *22*, 1010. (e) Day, V. W.; Klemperer, W. G.; Mainz, V. V.; Millar, D. M. *J. Am. Chem. Soc.* **1985**, *107*, 6262. (f) Hossain, M. A.; Hursthouse, M. B.; Malik, K. M. A. *Acta Crystallogr., Sect. B* **1979**, *B35*, 2258.
- (14) (a) Feher, F. J.; Budzichowski, T. A.; Rahimian, K.; Ziller, J. W. *J. Am. Chem. Soc.* **1992**, *114*, 3859. (b) Duchateau, R.; Cremer, U.; Harmsen, R. J.; Mohamad, S. I.; Abbenhuis, H. C. L.; van Santen, R. A.; Meetsma, A.; Thiele, S. K.-H.; van Tol, M. F. H.; Kranenburg, M. *Organometallics* **1999**, *18*, 5447. (c) Duchateau, R.; Abbenhuis, H. C. L.; van Santen, R. A.; Meetsma, A.; Thiele, S. K.-H.; van Tol, M. F. H. *Organometallics* **1998**, *17*, 5663. (d) Duchateau, R.; Abbenhuis, H. C. L.; van Santen, R. A.; Thiele, S. K.-H.; van Tol, M. F. H. *Organometallics* **1998**, *17*, 5222. (e) Edelmann, F. T.; Giessmann, S.; Fischer, A. *J. Organomet. Chem.* **2001**, *620*, 80. (f) Edelmann, F. T.; Giessmann, S.; Fischer, A. *Chem. Commun.* **2000**, 2153.

Cp^*TiCl_3 or $Ti(OR)_4$ and an incompletely condensed silsesquioxane or silanetriol, respectively. However, the framework Si:Ti ratio obtained in each of these two types of cubic titanosiloxanes is different; while the use of silsesquioxane results in a titanosiloxane **G** with a 7:1 Si:Ti ratio,^{14a} the use of silanetriol produces the titanosiloxane **H** with 1:1 Si:Ti ratio.^{13a} While it can be argued that the former compound **G** is an excellent model for the metal incorporated silica surfaces, the latter compound has the potential of being used as precursor for the preparation of titanosilicate materials with high titanium content, if the separation of TiO_2 phases could be avoided during its conversion to materials.

The TiO_2 phase separation from titanosilicate materials is normally expected in cases where either simple mononuclear precursors such as $Ti(OR)_4$ are used as titanium source or when the titanium content is in excess of 2–5% (e.g. synthesis of TS-1 and TS-2 type materials using $Ti(OPr^i_4)$).^{10a} Hence, it was thought in this study that a preformed titanosiloxane cage such as **H** with an exceptionally stable $Ti_4Si_4O_{12}$ core would in fact be converted into titanium-rich

- (15) (a) Coles, M. P.; Lugmair, C. G.; Terry, K. W.; Tilley, T. D. *Chem. Mater.* **2000**, *12*, 122. (b) Terry, K. W.; Tilley, T. D. *Chem. Mater.* **1991**, *3*, 1001. (c) Jarupatrakorn, J.; Tilley, T. D. *J. Am. Chem. Soc.* **2002**, *124*, 8380.

Scheme 1. Synthesis and Reactivity of $[\text{RSiO}_3\text{Ti}(\text{OPr}^i)]_4$ (**1**) and Its Conversion to $[\text{RSiO}_3\text{Ti}(\text{OBu}^t)]_4$ (**2**) ($\text{R} = 2,6\text{-Pr}_2\text{C}_6\text{H}_3\text{NSiMe}_3$)

titanosilicates without breaking the central core structure during decomposition at relatively low temperatures ($<500^\circ\text{C}$). Somewhat similar examples, using preformed titanosiloxanes as precursors for the preparation of titanium-rich titanosilicates, have been described recently. For example, Tilley et al. have demonstrated the applicability of the mononuclear titanium siloxide complex **A** in preparing $\text{TiO}_2 \cdot 4\text{SiO}_2$ materials by a thermolysis route and their use in olefin oxidation reactions.¹⁵ Similarly, Fujiwara and Roesky have shown that catalytically useful titanosilicate materials can be derived from a combination of cubic titanosiloxanes **H** and ~ 100 -fold tetraethyl orthosilicate through sol-gel routes in acetic anhydride medium.¹⁶ The utility of titanosilsesquioxane **G** as both homogeneous and heterogeneous oxidation catalysts has also been investigated.¹⁷

Although the cubic titanosiloxanes derived from discrete silanetriols were reported nearly a decade ago by Roesky et al.,^{13b} there has been no studies on further functionalization of these cubic structures at titanium and silicon corners.¹⁸ In the present investigation, continuing our studies on metal siloxanes and phosphates,¹⁹ we have investigated the reac-

tions of cubic titanosiloxane $[\text{RSiO}_3\text{Ti}(\text{OPr}^i)]_4$ ($\text{R} = 2,6\text{-Pr}_2\text{C}_6\text{H}_3\text{NSiMe}_3$) (**1**) with monosilanol $(\text{Bu}^t\text{O})_3\text{SiOH}$ and isolated a transesterification product which has been obtained through the hydrolysis of the monosilanol used. Further we have also investigated, in detail, the thermal decomposition of **1** leading to the isolation of titanium-rich titanosilicate materials. The use of these materials as epoxidation catalysts has also been probed. The details of these studies are presented in this paper.

Results and Discussion

Reactivity Studies. To study the reactivity of cubic titanosiloxanes, we chose $[\text{RSiO}_3\text{Ti}(\text{OPr}^i)]_4$ ($\text{R} = 2,6\text{-Pr}_2\text{C}_6\text{H}_3\text{NSiMe}_3$) (**1**)^{13a} for the reasons of high yields of the reaction and the relatively stable nature of the parent silanetriol.^{2b} This compound also has eight reactive functionalities at the eight corners of the cubic structure. While it has been well documented that the N-Si group of the silanetriol cleaves over a period of time in the presence of either an acidic/basic or highly polar medium,²⁰ the Ti-OR linkage is also known to undergo substitution as well as hydrolytic cleavage reactions.^{13c,16b} Considering the reactive nature of these linkages, it can be expected that any acidic hydrogen containing compound (alcohols, diols, phenols, carboxylic acids, etc.) would react with **1** to give a substituted compound at the titanium center. However these cubic molecules are highly stable under laboratory conditions and can be easily handled in air, suggesting that these hydrolyzable groups require forcing conditions for modifications at the corners of the cube.

On the other hand, the modification of these cubic structures with more exo-cubic silicon centers would also aid the usage of these molecules as single-source precursors

- (16) (a) Fujiwara, M.; Wessel, H.; Park, H. S.; Roesky, H. W. *Chem. Mater.* **2002**, *14*, 4975. (b) Fujiwara, M.; Wessel, H.; Park, H. S.; Roesky, H. W. *Tetrahedron* **2002**, *58*, 239.
- (17) (a) Abbenhuis, H. C. L.; Krijnen, S.; van Santen, R. A. *Chem. Commun.* **1997**, 331. (b) Krijnen, S.; Abbenhuis, H. C. L.; Hanssen, R. W. J. M.; van Santen, R. A. *Angew. Chem., Int. Ed.* **1998**, *37*, 356. (c) Wada, K.; Nakashita, M.; Bundo, M.; Ito, K.; Kondo, T.; Mitsudo, T. *Chem. Lett.* **1998**, 659.
- (18) While this work was under progress, Jutzi and co-workers have reported on the reactions of $\text{Cp}^*\text{Si}(\text{OH})_3$ -derived cubic titanosiloxanes with a range of reagents such as acetyl acetone, triphenyl silanol, etc. (see refs 13c,d).
- (19) (a) Sathiyendiran, M.; Murugavel, R. *Inorg. Chem.* **2002**, *41*, 6404. (b) Murugavel, R.; Walawalkar, M. G.; Prabusankar, G.; Davis, P. *Organometallics* **2001**, *20*, 2639. (c) Murugavel, R.; Prabusankar, G.; Walawalkar, M. G. *Inorg. Chem.* **2001**, *40*, 1084. (d) Murugavel, R.; Sathiyendiran, M. *Chem. Lett.* **2001**, *1*, 84. (e) Murugavel, R.; Sathiyendiran, M.; Walawalkar, M. G. *Inorg. Chem.* **2001**, *40*, 427. (f) Walawalkar, M. G. *Organometallics* **2003**, *22*, 879.

- (20) Voigt, A.; Walawalkar, M. G.; Murugavel, R.; Roesky, H. W.; Parisini, E.; Lubini, P. *Angew. Chem., Int. Ed. Engl.* **1997**, *36*, 2203.

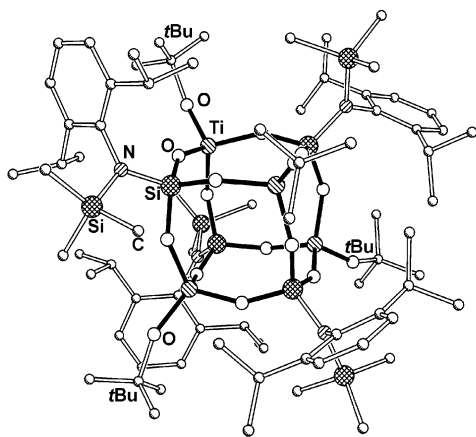


Figure 1. Molecular structure of $[\text{RSiO}_3\text{Ti}(\text{OBu}^t)]_4$ (**2**).

for the preparation of new titanosilicate materials. Hence, with this aim, the reaction of **1** with $(\text{Bu}^t\text{O})_3\text{SiOH}$ was carried out (Scheme 1). Although, it was originally expected that the $-\text{OPr}^i$ groups on titanium will be exchanged with $-\text{OSi}(\text{OBu}^t)_3$ groups, the final product obtained from the reaction mixture, after its crystallization over a period of 3 months, turned out to be $[\text{RSiO}_3\text{Ti}(\text{OBu}^t)]_4$ (**2**) instead of expected $[\text{RSiO}_3\text{Ti}(\text{OSi}(\text{OBu}^t)_3)]_4$.

A control experiment was carried out to evaluate the reactivity of titanosiloxane **1** with $(\text{Bu}^t\text{O})_3\text{SiOH}$ in a petroleum ether/toluene mixture for a period of 24 h at room temperature. At the end of the reaction the solvent was removed and the resultant residue was examined by electrospray LC-MS. The result obtained indicated that the silanol remains unreacted at the end of the reaction. Hence, it is reasonable to assume that formation of **2** proceeds via the cleavage of $\text{Si}-\text{OBu}^t$ group by hydrolysis from $(\text{Bu}^t\text{O})_3\text{SiOH}$ to form *tert*-butyl alcohol rather than from a preformed $[\text{RSiO}_3\text{Ti}(\text{OSi}(\text{OBu}^t)_3)]_4$. In fact we could not obtain any spectral evidence for the formation of $[\text{RSiO}_3\text{Ti}(\text{OSi}(\text{OBu}^t)_3)]_4$ during the course of the reaction. We have also performed an independent synthesis of **2** starting from **1** and a stoichiometric amount of Bu^tOH . The formation of product **2** was verified in this case by ^1H NMR spectroscopy.

Compound **2** was characterized by analytical, spectroscopic, and single-crystal X-ray diffraction studies. The crystals of **2** obtained directly from the reaction mixture were found to be analytically and spectroscopically pure. The characteristic infrared stretching frequency for $\text{Ti}-\text{O}-\text{Si}$ linkages was observed at 960 cm^{-1} . The aromatic and aliphatic stretching vibrations were observed in the region $3050\text{--}2850\text{ cm}^{-1}$. The ^1H NMR spectrum showed absence of the septet corresponding to the $-\text{CH}$ group of the $-\text{OPr}^i$ in **1** (δ 4.27 ppm); instead a new peak corresponding to the $-\text{OBu}^t$ appeared at (δ 1.6 ppm). The molecular ion peak observed for **2** in EI-MS spectrum (m/z 1782) confirms the exchange of the isopropyl group with the *tert*-butyl group.

X-ray Structures of 1 and 2. To explore the reactivity pattern and the effect of substituents on the structure of the cubic titanosiloxanes, we have carried out the single-crystal X-ray diffraction studies of compounds **1** and **2**. The compounds crystallize in cubic space group $I\bar{4}3d$ and are

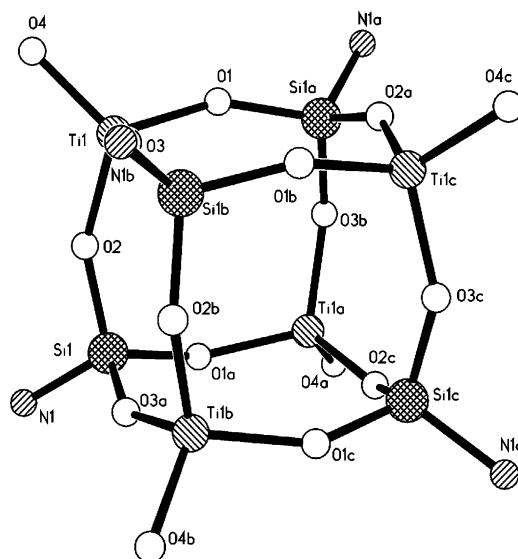


Figure 2. Core of molecule $[\text{RSiO}_3\text{Ti}(\text{OPr}^i)]_4$ (**1**).

Table 1. Selected Bond Lengths (Å) and Bond Angles (deg) for **1**^a

Ti(1)–O(4)	1.755(5)	Si(1)–O(1) ^{#2}	1.621(6)
Ti(1)–O(1)	1.807(5)	Si(1)–O(2)	1.618(5)
Ti(1)–O(2)	1.791(5)	Si(1)–N(1)	1.702(6)
Ti(1)–O(3)	1.807(5)	Si(2)–N(1)	1.756(6)
Si(1)–O(3) ^{#1}	1.619(5)		
O(4)–Ti(1)–O(1)	109.3(3)	O(1) ^{#2} –Si(1)–O(2)	106.7(3)
O(4)–Ti(1)–O(2)	112.3(3)	O(3) ^{#1} –Si(1)–N(1)	108.3(3)
O(1)–Ti(1)–O(2)	108.7(3)	O(1) ^{#2} –Si(1)–N(1)	113.9(3)
O(4)–Ti(1)–O(3)	111.4(3)	O(2)–Si(1)–N(1)	109.7(3)
O(1)–Ti(1)–O(3)	109.2(2)	Si(1) ^{#3} –O(1)–Ti(1)	148.0(3)
O(2)–Ti(1)–O(3)	106.1(2)	Si(1)–O(2)–Ti(1)	154.5(3)
O(3) ^{#1} –Si(1)–O(2)	111.4(3)	Si(1) ^{#1} –O(3)–Ti(1)	150.3(3)

^a Symmetry transformations used to generate equivalent atoms: #1, $-y + 11/4, x - 1/4, -z + 9/4$; #2, $-x + 3, -y + 5/2, z$; #3, $y + 1/4, -x + 11/4, -z + 9/4$.

Table 2. Selected Bond Lengths (Å) and Bond Angles (deg) for **2**^a

Ti(1)–O(4)	1.741(8)	Si(1)–O(2)	1.627(9)
Ti(1)–O(1)	1.789(9)	Si(1)–N(1)	1.709(10)
Ti(1)–O(2)	1.797(9)	Si(2)–N(1)	1.752(10)
Ti(1)–O(3)	1.810(9)	O(1)–Si(1) ^{#3}	1.627(9)
Si(1)–O(3) ^{#1}	1.626(9)	O(3)–Si(1) ^{#1}	1.626(9)
Si(1)–O(1) ^{#2}	1.627(9)		
O(4)–Ti(1)–O(1)	109.2(4)	O(1) ^{#2} –Si(1)–O(2)	107.6(5)
O(4)–Ti(1)–O(2)	111.6(4)	O(3) ^{#1} –Si(1)–N(1)	107.4(5)
O(1)–Ti(1)–O(2)	108.7(4)	O(1) ^{#2} –Si(1)–N(1)	114.2(5)
O(4)–Ti(1)–O(3)	110.9(4)	O(2)–Si(1)–N(1)	109.6(5)
O(1)–Ti(1)–O(3)	109.5(4)	Si(1) ^{#3} –O(1)–Ti(1)	150.7(5)
O(2)–Ti(1)–O(3)	106.8(4)	Si(1)–O(2)–Ti(1)	149.2(6)
O(3) ^{#1} –Si(1)–O(2)	112.4(5)	Si(1) ^{#1} –O(3)–Ti(1)	151.2(6)

^a Symmetry transformations used to generate equivalent atoms: #1, $-x + 3, -y + 5/2, z$; #2, $-y + 11/4, x - 1/4, -z + 9/4$; #3, $y + 1/4, -x + 11/4, -z + 9/4$.

isomorphous. A perspective view of the molecular structure of $[\text{RSiO}_3\text{Ti}(\text{OBu}^t)]_4$ (**2**) is shown in the Figure 1. The cubic core structure of **1** is shown in Figure 2. Selected bond lengths and bond angles found in **1** and **2** are listed in Tables 1 and 2, respectively. A comparison of the selected structural features of **1** and **2** with those of related titanosiloxanes is presented in Table 3.

The molecular structures of both **1** and **2** are made up of a $\text{Ti}-\text{O}-\text{Si}$ cubic framework with alternating titanium and silicon centers in the core (Figure 1). The $\text{Ti}_4\text{Si}_4\text{O}_{12}$

Table 3. Comparison of Key Structural Parameters in Cubic Titanosiloxanes Derived from Silanetriols^a

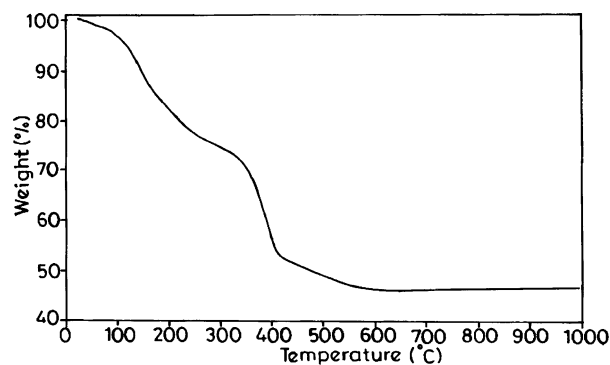
compd	Ti–O, Å	Si–O, Å	Ti–Si, Å	body diagonal, Å	Si–O–Ti, deg	ref
[RSiO ₃ Ti(MeC ₅ H ₄) ₄], R = Bu ^t	1.79	1.61	3.32	5.70	145–155	13b
[RSiO ₃ Ti(OEt) ₄], R = 2,6-Pr ₂ C ₆ H ₃ NSiMe ₃	1.80	1.63	3.32	5.75	145–155	13a
[RSiO ₃ Ti(OBu ^t) ₄], R = Cp [*]	1.78	1.62	3.33	5.74	136–158	13c
[RSiO ₃ Ti(OBu ^t) ₄], R = 9-(Me ₃ Si)fluorenyl	1.80	1.63	3.30	5.73	137–163	13d
[RSiO ₃ Ti(OPr ⁱ) ₄], R = 9-(Me ₃ Si)fluorenyl	1.79	1.62	3.31	5.73	138–165	13d
[RSiO ₃ Ti(OBu ^t) ₄], R = Bu ^t (Me ₃ Si)fluorenyl	1.77	1.63	3.33	5.72	141–158	13d
[RSiO ₃ Ti(OPr ⁱ) ₄], R = 2,6-Pr ₂ C ₆ H ₃ NSiMe ₃	1.80	1.62	3.32	5.75	148–154	this work
[RSiO ₃ Ti(OBu ^t) ₄], R = 2,6-Pr ₂ C ₆ H ₃ NSiMe ₃	1.79	1.62	3.33	5.72	146–154	this work
[(MeO)SiO _{1.5}] ₈ ^b		1.60	3.09 ^c	5.38	145–151 ^d	13e
[PhSiO _{1.5}] ₈ ^b		1.61	3.10 ^c	5.38	144–151 ^d	13f

^a Average values found in the core are listed. ^b This entry aids a direct structural comparison between cubic titanosiloxanes and cubic siloxanes. ^c The distance of the Si–Si edge. ^d Si–O–Si angle.

polyhedron (Figures 1 and 2) is completely enclosed in a hydrophobic sheath of alkyl-substituted aryl and SiMe₃ groups, which explains the high solubility of the cubic structures in hydrocarbon solvents. Each Si–Ti edge of the cube is bridged by an oxygen atom in a μ_2 fashion. There are six puckered Si₂Ti₂O₄ eight-membered rings that define the cube. Each of these rings adopts a pseudo-C₄ crown conformation. The four oxygen atoms on any of these six eight-membered rings are in a plane while the Ti and Si atoms form an almost parallel plane.

The average Ti–O bond length in the cubic framework (1.790(5) Å) is longer than the exocyclic Ti–O distance of 1.755(5) Å (Tables 1 and 2). These values are comparable to the Ti–O distances found in other cubic titanosiloxanes (Table 3). The average Si–O distance found in **1** (1.619(9) Å) is comparable with the corresponding distances found in other cubic titanosiloxanes (Table 3). The Si(1)–N(1) distance of 1.702(6) Å is considerably shorter than the Si(2)–N(1) distance of 1.756(6) Å. This observation is consistent with the presence of four electronegative atoms attached to Si(1). The observed short Si(1)–N(1) and Si(1)–O_{cage} distances could also be attributed to the multiple bonding resulting from negative hyperconjugative interactions (N_{1p}→Si–X σ^* and O_{1p}→Si–X σ^* type interactions where X = O or N).^{21–23} Such *cumulative* interactions leading to short C–O distances in the case of orthocarbonates C(OR)₄ has been demonstrated using extensive crystallographic investigations as well as ab initio quantum mechanical calculations.²³ Similar effects have also been observed for phosphinimines and iminophosphonium ions.^{21b} The SiO₃N coordination environments around the framework silicon atoms of the cube are very similar to orthocarbonates and phosphinimes, and hence, the observed Si–N and Si–O distances are attributable to enhanced cumulative hyperconjugative interactions.²⁴

It is of interest to calculate and compare the dimensions of the central cubic framework with related siloxanes. The

**Figure 3.** TGA trace for [RSiO₃Ti(OPrⁱ)₄ (**1**).

average length of the Si–Ti edge of the cube is 3.32 Å whereas the body diagonal of the Si₄Ti₄ cube is 5.75 Å (Table 3). These distances compare very well with those observed for other titanosiloxanes. The framework Si–O–Ti angles in **1** (148.0(3), 154.5(3), and 150.3(3)°) are also comparable to the values found in other cubic titanosiloxanes. The Ti and Si atoms adopt nearly ideal tetrahedral geometries (average angles around each of them being 109.5°). The sum of the angles around the nitrogen atom in **1** (359.9°) corresponds to a trigonal-planar geometry, which is also an expected requisite for negative hyperconjugative interactions leading to short Si–N distances. A comparison of the observed structural features of cubic titanosiloxanes with those of [(MeO)SiO_{1.5}]₈^{13e} and [PhSiO_{1.5}]₈^{13f} reveals that the core of the all-silicon cube in these molecules is approximately 10% smaller than their titanosiloxane counterparts (Table 3).

Thermal Decomposition Studies. To find the suitability of the cubic titanosiloxanes as single-source precursors for the preparation of titanium-rich titanosilicate materials, the thermogravimetric (TG) analysis of **1** was carried out. The initial TG analysis of **1** in air showed an onset temperature of decomposition at 140 °C which continued till 650 °C in stages (Figure 3), although no specific assignments could be made to the stepwise loss of the various organic substituents present on the surface of **1**. The ceramic yield obtained after heating **1** to 650 °C (46.1%) corresponds to the formation of TiO₂·2SiO₂ (theoretical yield 46.3%). This

- (21) (a) Murugavel, R.; Krishnamurthy, S. S.; Chandrasekhar, J.; Nethaji, M. *Inorg. Chem.* **1993**, *32*, 5447. (b) Murugavel, R.; Kumaravel, S. S.; Krishnamurthy, S. S.; Nethaji, M.; Chandrasekhar, J. *J. Chem. Soc., Dalton Trans.* **1994**, 847. (c) Murugavel, R.; Palanisami, N.; Butcher, R. J. *J. Organomet. Chem.* **2003**, *675*, 65. (d) Murugavel, R.; Pothiraja, R. *New J. Chem.* **2003**, *27*, 968.
- (22) (a) Lehn, J. M.; Wipff, G. *J. Chem. Soc., Chem. Commun.* **1975**, 800. (b) Reed, A. E.; Schleyer, P. v. R. *J. Am. Chem. Soc.* **1990**, *112*, 1434.
- (23) Narasimhamurthy, N.; Manohar, H.; Samuelson, A. G.; Chandrasekhar, J. *J. Am. Chem. Soc.* **1990**, *112*, 2937.

- (24) A manifestation of such cumulative interactions leading to short Si–O distances can also be seen in the silanol series bearing one, two, and three Si–OH groups: (PhCH₂)₃SiOH, 1.70(1) Å; (Bu^t)₂Si(OH)₂, 1.65(3) Å; Bu^tSi(OH)₃, 1.622(4) Å.

observation clearly suggests that, apart from the cubic framework silicon atoms in **1**, the exo-cubic $-\text{SiMe}_3$ groups are also converted into SiO_2 during thermal decomposition. The TGA showed no further weight loss until 1000 °C, revealing the complete removal of all organic groups in the temperature range 500–600 °C. Using the data obtained from TG studies, a bulk decomposition of the cubic titanosiloxane **1** was carried out at 450 (**1a**), 600 (**1b**), 800 (**1c**), 900 (**1d**), 1000 (**1e**), and 1200 °C (**1f**). The initial thermal decomposition at 450 °C produced a beige-colored material, whose elemental analysis showed the presence of carbon (0.5%) and hydrogen (1.3%) impurities. However, the same sample on calcination in air at 600 °C produced a white powder. The elemental analysis of this material showed no residual carbon. The presence of small quantities of hydrogen (0.7%) in this sample is attributed to the adsorption of water molecules on the titanosilicate material after calcination (which is also confirmed by independent IR studies; vide infra). There was no change in color or overall composition of the material on further calcination at temperatures up to 1200 °C.

At this point, it was necessary to ascertain the exact composition of the material and also verify the material yield obtained by TGA corresponding to the composition $\text{TiO}_2 \cdot 2\text{SiO}_2$. Hence, the titanium and silicon content in the material were determined using the acid digestion method recently reported by Gunji et al. (see Experimental Section).²⁵ The results obtained by this procedure revealed the titanium-to-silicon ratio to be 1:2.

The calcined samples at various temperatures (**1a–f**) were further investigated by powder X-ray diffraction (Figure 4) and infrared spectroscopic studies (Figure 5). While PXRD was very useful in assessing the crystalline nature of the material and the identification of the phases, IR spectroscopy has provided useful information about the presence or absence of relevant linkages in the material.²⁶ For example, the strong absorption in the IR spectrum observed around 960 cm^{-1} in titanosiloxane molecules as well as titanosilicate materials has been attributed to the presence of a Ti–O–Si linkage in the system.^{13a,26} In fact, the intensity of this absorption is often related to the extent of titanium incorporation into the framework of a titanosilicate material with Ti–O–Si linkages,^{26b,c} especially in the case of titanosilicate material with higher titanium content (e.g. >5%). Since, our TGA and solid-state decomposition studies point to the formation of $\text{TiO}_2 \cdot 2\text{SiO}_2$ material, it is of interest to study the intensity of 960 cm^{-1} absorption. The IR spectra of all the calcined samples, shown in Figure 5, clearly contain this absorption. However, it is instructive to note that the intensity of this absorption decreases with increase in the calcination temperature indicating a probable phase separation of TiO_2 from the titanosilicate materials at higher temperature. Thus,

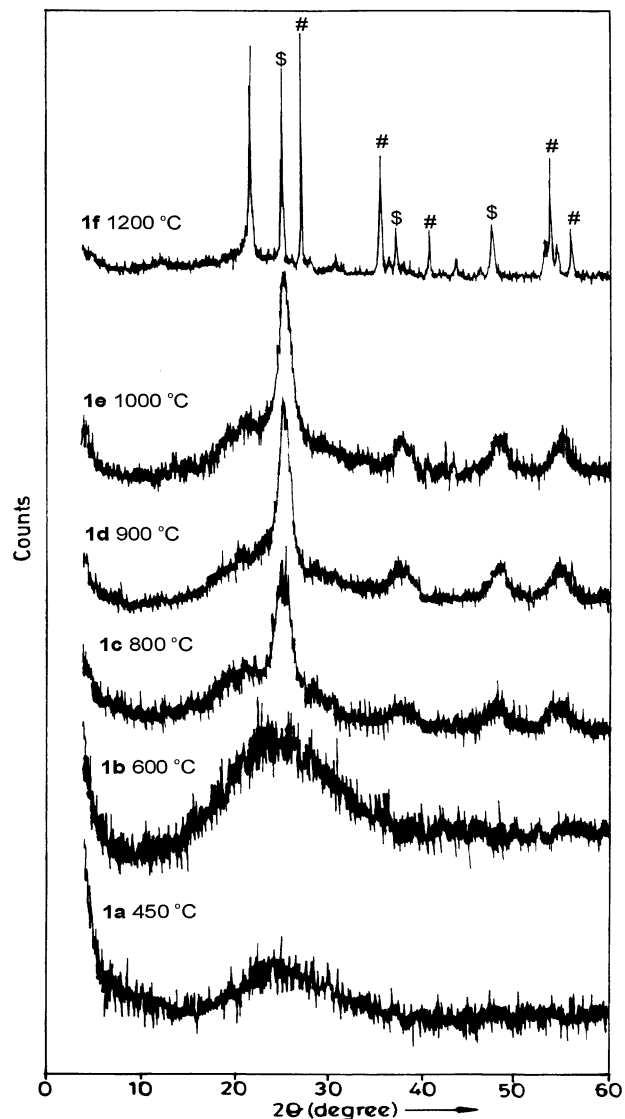


Figure 4. Powder XRD patterns of **1a–f**. The peaks due to anatase- TiO_2 are marked \$ while the peaks due to rutile form are labeled #. The unindexed peaks found in **1f** are due to a crystalline titanosilicate material.

it can be concluded that when the decomposition is carried out at relatively lower temperature, the presence of Ti–O–Si linkages in the ceramic material is observed, and on increasing the temperature above 800 °C, the Ti–O–Si linkages break down to form TiO_2 phases. This observation also suggests that the compound **1** does not retain its central cubic core in the titanosilicate materials, at least those produced at high temperatures.

The presence of a strong broad absorption ca. 3400 cm^{-1} in samples **1a–f** is attributed to the adsorption of water molecules on the titanosilicate material during sample preparation for spectral studies. The powder X-ray diffraction of **1a** (Figure 4) does not show any peaks revealing the complete amorphous nature of the material. Subsequent heating of the sample at 600 °C (**1b**) also failed to introduce any kind of crystallinity to the material. The material heated at 800 °C for 4 h (**1c**) showed four broad peaks and a broad band overlapping with the highest peak. This could be attributed to the crystallization of titanosilicate material (vide infra). To study the crystallization behavior in detail, the

(25) Gunji, T.; Kubota, K.; Kishiki, S.; Abe, Y. *Bull. Chem. Soc. Jpn.* **2002**, *75*, 537.

(26) (a) Uguina, M. A.; Ovejero, G.; van Grieken, R.; Serrano, D. P.; Camacho, M. *J. Chem. Soc., Chem. Commun.* **1994**, 27. (b) Hutter, A.; Dutoit, D. C. M.; Mallat, T.; Schneider, M.; Baiker, A. *J. Chem. Soc., Chem. Commun.* **1995**, 163. (c) Dutoit, D. C. M.; Mallat, T.; Baiker, A. *J. Catal.* **1995**, *153*, 177.

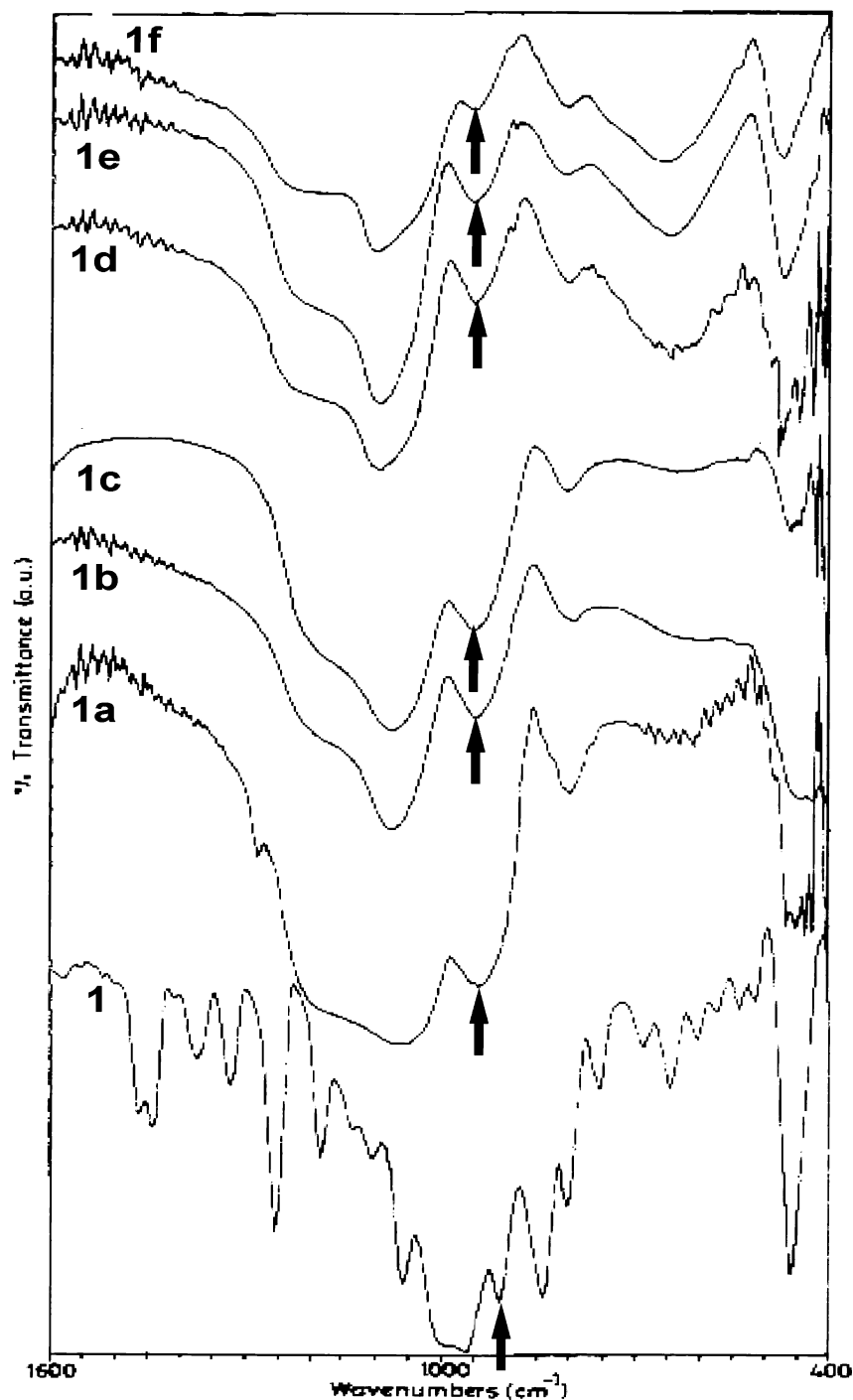


Figure 5. Infrared spectrum of $[\text{RSiO}_3\text{Ti}(\text{OPr})_4]$ (**1**) and the calcined samples (in KBr). The peaks at 960 cm^{-1} due to the Ti–O–Si vibration are shown with arrows.

sample was subsequently heated at 900 (**1d**), 1000 (**1e**), and $1200\text{ }^\circ\text{C}$ (**1f**). The powder XRD pattern of both **1d,e**, show the sharpening of the broad peak ($2\theta = 25.4^\circ$) and also the emergence of four new distinct peaks, which can be indexed to the anatase phase of TiO_2 ($2\theta = 25.3$ and 37.8°). However, the sample **1f** is fully crystalline, gave five distinct major peaks in powder XRD analysis. The peaks observed at $2\theta = 25.5, 37.9, 48.2,$ and 55.3° can be indexed to the anatase phase,^{27a} whereas the peaks at $2\theta = 27.7, 36.3, 39.4, 41.5, 44.3, 54.0, 54.5,$ and 56.8° correspond to the rutile phase of TiO_2 .^{27b} This is clearly indicative of the phase separation

occurring in the sample due to the breakdown of Ti–O–Si linkages of **1** during the calcination process. It appears that the unindexed lines in the XRD pattern of the sample **1f**, shown in Figure 4, correspond to a titanosilicate phase, which also accounts for the residual Ti–O–Si absorption at 960 cm^{-1} in its IR spectrum (Figure 5).

UV–vis spectroscopy has also been used to characterize the materials **1a–f**. The electronic absorption observed in

(27) (a) Rausch, N.; Burte, E. P. *J. Electrochem. Soc.* **1993**, *140*, 145. (b) Ritala, M.; Leskela, M.; Nykanen, E.; Soininen, P.; Niinisto, L. *Thin Solid Films* **1993**, *225*, 288.

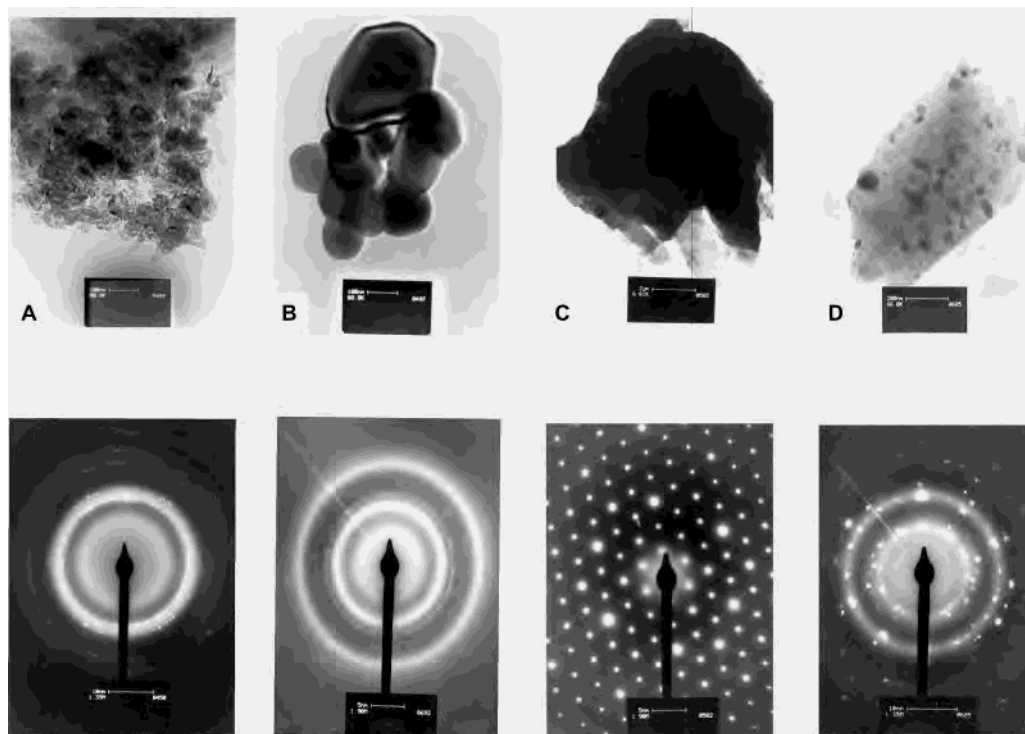


Figure 6. Top: TEM bright-field micrographs of the samples **1c** (A), **1d** (B), **1e** (C) and **1f** (D). Bottom: Corresponding electron diffraction pattern of a chosen particle from the respective samples.

titanosilicates could be due to the charge transfer between the oxide ions of the lattice and an empty d-orbital of the Ti(IV).^{26,28} The position of the absorption maximum of tetrahedral and octahedral Ti(IV) is normally expected at 45 000–48 000 and 42 000 cm^{-1} , respectively. The absorbance maxima for the titanium containing materials **1a–f** were broadened and shifted to lower wavelengths (33 100 cm^{-1}). This is consistent with the presence of octahedral Ti sites. In fact, the presence of octahedral sites within the silica matrix is expected to be from higher titanium content (> ca. 8 mol % as described in the literature).^{26,28}

The surface and morphology of the materials **1a–f** were examined using scanning electron microscopy (SEM). The SEM micrograph of sample **1a** depicts irregularity in the crystalline nature of the surface. As the calcination temperature is increased, the particles become more crystalline. For example, sample **1e** shows the maximum amount of regularity of the surface. The microstructures of the materials **1c–f** were further studied using transmission electron microscopy (TEM) (Figure 6). The particle size of sample **1c** varies from 35 to 80 nm in diameter. The ring pattern obtained from TEM electron diffraction study for sample **1c** reveals the polycrystalline nature of the material. The material **1d** also shows a similar behavior (Figure 6; sample B). Sample **1e**, which is heated at 1000 °C, is the most crystalline product, and its particle size ranges from 85 to 115 nm. The microdiffraction of the material shows both ring pattern as well as spot pattern at various regions. Ring pattern is due to the presence of polycrystalline material or a thick sample containing single crystals, whereas the spot pattern (Figure

6; sample C) is from a highly crystalline phase. The TEM images of sample **1f** show a ring as well as a spot pattern at different regions (Figure 6; sample D). This reveals the presence of amorphous, polycrystalline, and single-crystalline titanosilicates in the same material. The energy-dispersive X-ray analyses (EDAX) of the samples **1a–f** show the presence of Ti and Si in an approximate ratio of 1:2, further confirming our results obtained for titanium content through the acid digestion method (vide supra). Further work is necessary to clearly understand the exact microstructure of these materials and the surface characteristics such as surface area and porosity.

Cyclohexene Epoxidation. Titania–silica mixed oxides and titanosilicates such as TS-1 and TS-2 are effective catalysts for epoxidation and selective oxidation reactions using peroxides as oxidants.²⁹ The active sites are assumed to be the isolated tetrahedral Ti^{4+} centers.^{29c} The presence of polar solvents greatly retards the reaction by competing for the active coordination sites.³⁰ Highly dispersed titania–silica is very effective for olefin epoxidation with alkyl hydroperoxides. The formation of Ti–O–Si bonds is very crucial as demonstrated by the much lower activities of TiO_2 supported on other oxides and the physical mixtures of TiO_2 and SiO_2 .^{28,29b,c,30}

- (28) (a) Shraml-Marth, M.; Walther, K. L.; Wokaun, A.; Handy, B. E.; Baiker, A. *J. Non-Cryst. Solids* **1992**, *143*, 93.
 (29) (a) Reddy, J. S.; Kumar, R.; Ratnasamy, P. *App. Catal.* **1990**, *58*, L1. (b) Maschmeyer, T.; Klunduk, M. C.; Martin, C. M.; Shephard, D. S.; Thomas, J. M.; Johnson, B. F. G. *Chem. Commun.* **1997**, 1847. (c) Sheldon, R. A.; van Doorn, J. A. *J. Catal.* **1973**, *31*, 427. (d) Notari, B. *Catal. Today* **1994**, *18*, 163.
 (30) (a) Gao, X.; Wachs, I. E. *Catal. Today* **1999**, *51*, 233. (b) Blasco, T.; Corma, A.; Navarero, M. T.; Pérez-Pariente, J. *J. Catal.* **1995**, *156*, 65. (c) Thomas, J. M. *Chem.–Eur. J.* **1997**, *3*, 1557. (d) Beghi, M.; Chiurlo, P.; Costa, L.; Palladino, M.; Pirini, M. F. *J. Non-Cryst. Solids* **1992**, *145*, 175. (e) Klein, S.; Weckhuysen, B. M.; Martens, J. A.; Maier, W. F.; Jacobs, P. A. *J. Catal.* **1996**, *163*, 489.

(28) (a) Shraml-Marth, M.; Walther, K. L.; Wokaun, A.; Handy, B. E.; Baiker, A. *J. Non-Cryst. Solids* **1992**, *143*, 93.

Table 4. Conversion of Cyclohexene to Cyclohexene Oxide

no.	catal	% conversion
1	1 ^a	15
2	1b	11
3	1c	11
4	1d	1
5	1e	1

^a Used as a homogeneous catalyst.

Owing to the presence of a number Ti–O–Si linkages with tetrahedral titanium, the catalytic performances of the molecular precursor, [RSiO₃Ti(OPr^f)₄] (1), and titania–silica materials (**1b–e**) were studied toward the epoxidation of cyclohexene. Compound **1a** was not used in the catalytic studies due to its residual carbon content while the catalytic activity of **1f** was not investigated because of the larger TiO₂ phase separation in this sample. All epoxidation reactions were carried out in toluene at 65 °C with cumenyl hydroperoxide as oxidant. The conversion of cyclohexene to cyclohexene oxide was followed by GC-MS. To compare the activities, the results were standardized with respect to the mass of the catalyst used. In the control experiments carried out with **1** in the absence of hydroperoxide, a negligible amount of cyclohexene oxide product was observed by GC analysis after 23 h. Similarly, the heterogeneous catalysts **1a–f** also in the absence of hydroperoxide did not show any appreciable activity.³¹

The molecular precursor **1** was found to be an active homogeneous catalyst for the epoxidation of cyclohexene (15% conversion) after 23 h (Table 4). Epoxidation using heterogeneous titania–silica materials **1b–e** was also carried out under similar conditions. It is found that the samples **1b,c** show ~11% conversion. Cyclohexene oxide was the sole product in all these cases, thus showing a very high selectivity in the epoxidation process. However, the samples **1d,e** gave a conversion of only <1%. The drastic decrease in catalytic performance in the latter case is attributed to the phase separation of TiO₂ occurring in the material at elevated temperatures. This observation is also consistent with the reduction in the intensity of Ti–O–Si vibration at 960 cm⁻¹ (Figure 5) due to the formation of significant amount of TiO₂. Powder XRD and DR UV measurements also support this TiO₂ phase separation hypothesis for the reduced catalytic activity of **1d,e**. At low temperatures of calcination, the tetrahedral titanium center predominates whereas at higher temperatures of calcination octahedral titanium centers were formed.

The results obtained from the above-described reactions are in fact difficult to understand since the increased titanium content in **1a–f** did not lead to a better conversion of cyclohexene to its epoxide. Possible reasons for the decreased catalytic efficiency could be either due to the presence of too many tetrahedral titanium centers in close proximity (crowding) or the coexistence of small amounts of TiO₂ phase with octahedral titanium centers along with the

titanosilicates (irrespective of the temperature used for the decomposition). Alternatively, the low conversion could also be attributed to rapid catalytic peroxide decomposition. Hence, it is necessary to investigate the catalysis aspects of **1a–f** further in detail and also understand the surface characteristics of these materials before any meaningful comparison could be made with the results obtained for other epoxidation catalysts based on titanosilicates. Hence, further experiments are necessary to optimize olefin epoxidation reactions in terms of the choice of substrate, choice of the oxidant, reaction temperature, and reaction time. Work in this direction is currently underway.

Conclusion

It has been shown in this contribution that the modification of the periphery of cubic titanosiloxanes occurs only at the titanium center over a period of time although the original objective of increasing the silicon content on the cubic titanosiloxane was unsuccessful. The compound [RSiO₃Ti(OPr^f)₄] undergoes in situ transesterification to form isomorphous molecule [RSiO₃Ti(OBu^f)₄]. We have shown that it is possible to prepare titanium-rich titanosilicate materials from soluble titanosiloxane molecules. The solid state thermolysis at relatively lower temperatures (<800 °C) leads to the formation of Ti–O–Si materials, which are shown to be potential catalysts for olefin epoxidation. However, the calcination of the titania–silica material at high temperatures (>800 °C) produced a mixture of titanosilicates along with phase-separated TiO₂, which shows lesser activity toward olefin epoxidation. Further work in our laboratory is centered on further functionalization of cubic titanosiloxanes as well as optimization of olefin epoxidation reactions using **1a–f**.

Experimental Section

Material and Methods. All manipulations were performed under an atmosphere of nitrogen using standard Schlenk techniques. Solvents used were freshly distilled prior to use. The silanetriol, RSi(OH)₃ (R = 2,6-Pr₂C₆H₃NSiMe₃),^{2b} and silanol, (Bu^fO)₃SiOH,³² have been synthesized by following the reported procedures. Ti(OPr^f)₄ obtained from E-Merck was used as received. Cumenyl hydroperoxide was procured from Lancaster (80% tech).

Chemical analysis has been carried out at the Analytical Laboratories of the Department of Chemistry, IIT-Bombay, Bombay, on a Carlo Erba model 1106 instrument. ¹H NMR spectra were recorded on a Varian VXR 400S spectrometer. Infrared spectrum of the samples were obtained on a Nicolet Impact 400 spectrometer. The DR UV spectra of the calcined samples were recorded on a Shimadzu UV-260 UV–vis spectrophotometer in the reflectance mode for the well-ground solid samples. The thermal analysis of the cubic titanosiloxane **1** has been carried out in air with the heating rate of 10 °C min⁻¹ on a DuPont model 2100 thermal analyzer. The powder X-ray diffraction studies were carried out on a Philips PW1729 X-ray diffractometer using Cu K α radiation. SEM work was done on a JEOL JSM-840A. Samples were prepared by ultrasonication in acetone and then dispersed on a copper stub. TEM micrographs were obtained on a Philips CM 200 microscope. As the samples show crystalline behavior only above 800 °C, the TEM measurements were carried out only for the samples **1c–f**. Progress

(31) Another control experiment carried out for the oxidation of cyclohexene in the presence of oxidant alone also produced no appreciable amounts of cyclohexene oxide.

(32) Abe, Y.; Kijima, I. *Bull. Chem. Soc. Jpn.* **1969**, *42*, 1118.

Table 5. Crystal Data and Structure Refinement for **1** and **2**

	1	2
empirical formula	C ₇₂ H ₁₃₂ N ₄ O ₁₆ Si ₈ Ti ₄	C ₇₆ H ₁₄₀ N ₄ O ₁₆ Si ₈ Ti ₄
fw	1726	1782
temp, K	293(2)	200(2)
wavelength, Å	0.710 73	0.710 73
cryst system, space group	cubic, <i>I</i> $\bar{4}$ 3 <i>d</i>	cubic, <i>I</i> $\bar{4}$ 3 <i>d</i>
unit cell dimens	<i>a</i> = 31.702	<i>a</i> = 31.606
<i>V</i> , Å ³	31 860.7	31 572.5
<i>Z</i>	12	12
calcd density, Mg/m ³	1.080	1.125
abs coeff, mm ⁻¹	0.430	0.436
<i>F</i> (000)	11 040	11 424
θ range for data collcn, deg	1.57–24.99	3.53–25.16
index ranges	0 ≤ <i>h</i> ≤ 37, 0 ≤ <i>k</i> ≤ 37, 0 ≤ <i>l</i> ≤ 37	0 ≤ <i>h</i> ≤ 37, 0 ≤ <i>k</i> ≤ 26, 0 ≤ <i>l</i> ≤ 37
reflens collcd/unique	14 237/2482 [R(int) = 0.0698]	4897/2478 [R(int) = 0.1292]
completeness to 2 θ , %	99.9	98.6
refinement method	full-matrix LS on <i>F</i> ²	full-matrix LS on <i>F</i> ²
data/restraints/params	2482/0/245	2478/0/255
goodness-of-fit on <i>F</i> ²	1.067	1.083
final R indices [<i>I</i> > 2 σ (<i>I</i>)]	R1 = 0.0520, wR2 = 0.1353	R1 = 0.0879, wR2 = 0.1753
R indices (all data)	R1 = 0.0919, wR2 = 0.1622	R1 = 0.1525, wR2 = 0.2307
largest diff peak and hole, e Å ⁻³	0.425 and -0.238	0.693 and -0.720

of the epoxidation reactions was monitored on a Perkin-Elmer Clarus GC-MS system. The metal content in the sample was determined by following the procedure of Gunji et al.²⁵

Synthesis of [RSiO₃Ti(OPr^{*i*})₄] (R = 2,6-Pr^{*i*}₂C₆H₃NSiMe₃) (1). ¹³a RSi(OH)₃ (1 g, 3.3 mmol) was suspended in petroleum ether (30 mL), and Ti(OPr^{*i*})₄ (1 mL, 3.3 mmol) was added slowly with stirring. The solution became clear on stirring for 4 h after which solvent was removed in vacuo, and the residue obtained was dried for 12 h and redissolved in minimum amount of petroleum ether. X-ray-quality crystals were grown at room temperature. The product was separated by decantation. Yield: 82% (1.02 g). Anal. Calcd C₇₂H₁₃₂N₄O₁₆Si₈Ti₄: C, 50.1; H, 7.7; N, 3.3. Found: C, 50.2; H, 8.4; N, 3.3. IR (KBr): 1321, 1248, 1183, 1097, 1064, 966, 913, 841, 802 cm⁻¹. ¹H NMR (300 MHz, CDCl₃): δ 0.09 (s, 36H, SiMe₃), 0.96 (d, 24H, Me₂), 1.16 (d, 24H, Me₂), 1.24 (d, 24H, Me₂), 3.52 (septet, 8H, CH), 4.27 (septet, 4H, OCH), 6.99 (s, 12H, Ph) ppm.

Synthesis of [RSiO₃Ti(OBu^{*t*})₄] (2). [RSiO₃Ti(OPr^{*i*})₄] (1) (1 g, 0.58 mmol) was dissolved in a 1:1 mixture of toluene/petroleum ether (20 mL), and (Bu^{*t*}O)₃SiOH (0.448 g, 2.32 mmol) in petroleum ether (10 mL) was slowly added to the above solution. The reaction mixture was stirred for 24 h. The solvent was concentrated to half the volume. Colorless X-ray-quality crystals were grown at room temperature over a period of 90 days. Yield: 40% (332 mg based on [RSiO₃Ti(OPr^{*i*})₄]). Anal. Calcd For C₇₆H₁₄₀N₄O₁₆Si₈Ti₄: C, 51.22; H, 7.91; N, 3.14. Found: C, 51.20; H, 7.85; N, 2.49. IR (KBr): 1443, 1255, 1083, 974, 909, 853, 802 cm⁻¹. ¹H NMR (300 MHz, C₆D₆): δ 0.05 (s, 36H, SiMe₃), 0.2 (d, 36H, Me₂), 1.16 (d, 24H, Me₂), 1.6 (d, 24H, Me₂), 3.52 (sep. 8H, CH), 6.99 (s, 12H, Ph) ppm. Mass spectrum (EI): *m/e* 1782 (M⁺).

Thermolysis of [RSiO₃Ti(OPr^{*i*})₄] (1a–f). A sample of [RSiO₃-Ti(OPr^{*i*})₄] (1) (1 g) was weighed in a platinum crucible and heated in air at 450 °C at a rate of 10 °C min⁻¹ for 4 h. The sample was allowed to cool to room temperature affording (0.45 g, 45%) a beige-colored solid. The material was subsequently calcined at various temperatures to get the different materials (600 °C (1b), 800 °C (1c), 900 °C (1d), 1000 °C (1e), and 1200 °C (1f)).

Estimation of Ti and Si. The titanium and silicon contents were determined by following a reported literature procedure.²⁵ For the estimation of TiO₂ and SiO₂, 0.2 g of the respective sample was weighed in a crucible and sulfuric acid (0.5 mL) was added. After gradual heating in a Kjeldahl flask overnight (until the evolution

of fume ceases), the residue was weighed (A). Independently, 0.2 g of the sample was weighed in a flask and heated in the presence of ammonium sulfate (1 g), ammonium nitrate (1 g), and sulfuric acid (20 mL) for 48 h. The residue was poured into 100 g of ice, followed by filtration. The residue was subjected to firing in a crucible, followed by weighing (B). The content of SiO₂ was calculated from the content (B), and the content of TiO₂ was calculated from the difference between the contents (A and B).

Epoxidation of Cyclohexene. Appropriate catalyst (50 mg), toluene (5 mL), and cyclohexene (2.5 mL, 24.7 mmol) were taken in a round-bottom flask. Reaction mixture was heated in an oil bath and allowed to equilibrate at 65 °C for 10 min. Cumenyl hydroperoxide (1 mL) was then added with stirring. The mixture was stirred for 23 h and allowed to attain room temperature. It was then centrifuged to remove the suspended particles of the catalyst. The samples were analyzed using GC-MS. A similar procedure was adopted for all other samples.

X-ray Structure Determination of 1 and 2. Single crystals of **1** and **2** suitable for X-ray structure analysis were grown using the procedure described vide supra. Intensity data for [RSiO₃Ti(OPr^{*i*})₄] (1) were collected on Nonius MACH-3 diffractometer. A Siemens-STOE AED2 four-circle diffractometer using Mo K α radiation at room temperature was used for **2**. Intensity data collection and cell determination for both the compounds were carried out using a monochromatized Mo K α radiation in the both diffractometers. Data were suitably processed, and the space group determination was carried out by examining the systematic absences. The structure solution in each case was achieved using SHELXS-97.³³ The refinement of the structure was carried out SHELXL-97.^{33,34} The positions of hydrogen atoms were geometrically fixed and refined using a riding model. All non-hydrogen atoms were refined anisotropically. Other details pertaining to data collection, structure solution, and refinement are given in Table 5. Atomic coordinates, complete bond distances and bond angles, and anisotropic thermal parameters of all non-hydrogen atoms are deposited as Supporting Information in the form of CIF files.

Acknowledgment. We acknowledge generous financial support by the DST, New Delhi, for carrying out this work

(33) Sheldrick, G. M. *SHELXS-97: Program for Crystal Structure Solution*; University of Göttingen: Göttingen, Germany, 1997.

(34) Sheldrick, G. M. *SHELXL-97: Program for Crystal Structure Refinement*; University of Göttingen: Göttingen, Germany, 1997.

in the form of a Swarnajayanti Fellowship Project to R.M. This work was also supported in part by a DAE Young Scientist Research Award to R.M. P.D. thanks the CSIR, New Delhi, for a senior research fellowship. The authors thank the DST-funded Single Crystal X-ray Diffractometer Facility at IIT-Bombay for the X-ray diffraction data for compound **1** and the RSIC, IIT-Bombay, for the TGA and TEM measurements. We thank the Department of Metallurgical Engineering and Materials Science, IIT Bombay, for powder XRD and the Department of Earth Sciences, IIT Bombay, for SEM studies. The authors thank the reviewers

of this manuscript for their comments, which were useful in revising the paper. R.M. thanks Prof. H. W. Roesky for introducing him to silanetriol chemistry and constant encouragement.

Supporting Information Available: X-ray data (including atomic coordinates, complete bond lengths and angles, anisotropic thermal parameters, and hydrogen atom coordinates) in CIF format for compounds **1** and **2**. This material is available free of charge via the Internet at <http://pubs.acs.org>.

IC034317M